Protein Science (1997), 6:1718–1726. Cambridge University Press. Printed in the USA.

Xylanase XynA from the hyperthermophilic bacterium *Thermotoga maritima*: Structure and stability of the recombinant enzyme and its isolated cellulose-binding domain

DORIS WASSENBERG,[1] HARTMUT SCHURIG,[1] WOLFGANG LIEBL,[2] AND RAINER JAENICKE[1]

[1]Institut für Biophysik und Physikalische Biochemie, Universität Regensburg, D-93040 Regensburg, Germany
[2]Lehrstuhl für Mikrobiologie, Technische Universität München, D-80290 München, Germany

(RECEIVED January 13, 1997; ACCEPTED April 21, 1997)

Abstract

The hyperthermophilic bacterium *Thermotoga maritima* is capable of gaining metabolic energy utilizing xylan. XynA, one of the corresponding hydrolases required for its degradation, is a 120-kDa endo-1,4-D-xylanase exhibiting high intrinsic stability and a temperature optimum ~90 °C. Sequence alignments with other xylanases suggest the enzyme to consist of five domains. The C-terminal part of XynA was previously shown to be responsible for cellulose binding (Winterhalter C, Heinrich P, Candussio A, Wich G, Liebl W. 1995. Identification of a novel cellulose-binding domain within the multi-domain 120 kDa Xylanase XynA of the hyperthermophilic bacterium *Thermotoga maritima*. *Mol Microbiol 15*:431–444).

In order to characterize the domain organization and the stability of XynA and its C-terminal cellulose-binding domain (CBD), the two separate proteins were expressed in *Escherichia coli*. CBD, because of its instability in its ligand-free form, was expressed as a glutathione S-transferase fusion protein with a specific thrombin cleavage site as linker. XynA and CBD were compared regarding their hydrodynamic and spectral properties. As taken from analytical ultracentrifugation and gel permeation chromatography, both are monomers with 116 and 22 kDa molecular masses, respectively. In the presence of glucose as a ligand, CBD shows high intrinsic stability. Denaturation/renaturation experiments with isolated CBD yield >80% renaturation, indicating that the domain folds independently. Making use of fluorescence emission and far-UV circular dichroism in order to characterize protein stability, guanidine-induced unfolding of XynA leads to biphasic transitions, with half-concentrations $c_{1/2}$(GdmCl) ~4 M and >5 M, in accordance with the extreme thermal stability. At acid pH, XynA exhibits increased stability, indicated by a shift of the second guanidine-transition from 5 to 7 M GdmCl. This can be tentatively attributed to the cellulose-binding domain. Differences in the transition profiles monitored by fluorescence emission and dichroic absorption indicate multi-state behavior of XynA. In the case of CBD, a temperature-induced increase in negative ellipticity at 217 nm is caused by alterations in the environment of aromatic residues that contribute to the far-UV CD in the native state.

Keywords: cellulose-binding domain; hyperthermophiles; stability; *Thermotoga maritima*; xylanase

The hyperthermophilic bacterium *Thermotoga maritima* is capable of utilizing simple carbohydrates as well as complex polysaccharides to gain energy. This includes xylan, which, besides cellulose, is one of the main components of secondary walls of plants. The amount of xylan varies from 7% of the dry weight of gymnosperms to 35% in birchwood (Whistler & Richards, 1970). The xylose backbone, of which the β-1,4-glycosidic bonds can be hydrolyzed by xylanases, usually carries various substituents, e.g., acetyl, arabinosyl, or uronyl side chains (Aspinall, 1980). Possible applications for xylanases in biotechnology are digestion of industrial and agricultural wastes, as well as reduction of the amount of required chemicals (chlorine) in paper pulp bleaching, thus reducing the release of, e.g., polychlorinated dibenzodioxins and dibenzofurans, suspected to be human carcinogens (Amato, 1993). Reprecipitated xylan on the surface of pulp fibers lowers the effectivity of bleaching; thus, hydrolyzing xylan improves the accessibility of bleaching agents to residual lignin, keeping the cellulose content constant (Kantelinen et al., 1993). These processes are optimally carried out at high temperatures, so it is highly desirable to search for hyperthermostable xylanases as catalysts.

Reprint requests to: Dr. Rainer Jaenicke, Institut für Biophysik und Physikalische Biochemie, Universität Regensburg, Universitätsstr. 31, D-93040 Regensburg, Germany; e-mail: rainer.jaenicke@biologie.uni-regensburg.de.

Abbreviations: CBD, cellulose-binding domain; CD, circular dichroism; *E. coli*, *Escherichia coli*; GdmCl, guanidinium chloride; GST, glutathione S-transferase; IPTG, isopropyl-β-D-thiogalactopyranoside; *T. maritima*, *Thermotoga maritima*; XynA, xylanase A

XynA, the 120-kDa endo-1,4-D-xylanase of *Thermotoga maritima* MSB8 has been purified and characterized by Winterhalter et al. (1995). With its temperature optimum at 90 °C, it is one of the most thermostable xylanases isolated so far.

As suggested by sequence comparison, the enzyme consists of five domains: The central catalytic domain shares amino acid sequence similarity with other xylanases of family 10 of glycosyl hydrolases and shows $(\alpha/\beta)_8$-barrel topology (Henrissat, 1991). The dissimilar N- and C-terminal parts of the protein consist of duplicated sequences of about two times 150 and two times 180 amino acids, respectively.

The intrinsic stability of thermostable xylanases has previously been ascribed to the N-terminal domains of the enzymes (Lee et al., 1993; Fontes et al., 1995; Winterhalter et al., 1995). The hypothesis was challenged after a homologous N-terminal sequence was discovered in the enzyme from the mesophilic bacterium *Cellulomonas fimi* (Clarke et al., 1996). However, after this was shown to exhibit a temperature optimum of its catalytic activity at 60 °C, the above assignment may still be valid.

The duplicated C-terminal domain belongs to a novel type of cellulose-binding domains (CBDs), also present in modular xylanases from *Thermoanaerobacterium saccharolyticum* (Lee et al., 1993), *Clostridium thermocellum* (M.Y. Pack & K.H. Jung, 1993, unpublished DNA sequence, available in EMBL nucleotide sequence database under accession number M67438), *Thermotoga neapolitana* (Zverlov et al., 1996), and the mesophilic *Cellulomonas fimi* (Clarke et al., 1996). It has been shown by Black et al. (1996) that CBDs enhance the activity of hemicellulases against complex substrates, e.g., plant cell walls, by promoting a closer contact to the substrate.

Here we report the preparation of the CBD of xylanase XynA of *Thermotoga maritima*. Aiming at thermodynamic data for the intrinsic stability, thermal and GdmCl-dependent unfolding was applied. On the other hand, denaturation/renaturation was used in the attempt to gain insight into the folding mechanism of the complex multi domain protein. In order to examine the mutual stabilization of the domains, the spectroscopic properties and the denaturation transitions of both CBD and the entire enzyme were investigated.

Results and discussion

Purification of the cellulose-binding domain

The C-terminal CBD of XynA from *T. maritima* was prepared by specific proteolysis of a fusion protein combining CBD with Glutathione S-transferase. The fusion protein was designed with a thrombin recognition site in the linker between CBD and GST (Fig. 1). In this context, it should be noted that the N-terminus of the isolated domain, as deduced from sequence alignment, is extended by six amino acid residues not present in the *T. maritima* sequence. Since the hexapeptide contains two Gly and two Pro residues, it may be assumed to be unstructured so that no significant contribution to the intrinsic stability of CBD is to be expected.

After expression of the fusion protein in *E. coli*, purification was accomplished by affinity chromatography on microcrystalline cellulose as described in Materials and methods. Proteolysis was optimized with respect to temperature, protease-substrate ratio, buffer conditions, and incubation time. Complete cleavage was reached after 16 h at room temperature in 50 mM sodium phosphate, pH 6.2 with a thrombin-substrate ratio of 1 U per mg. No unspecific proteolytic reactions could be observed under these conditions (Fig. 2). Purification of the domain made use of the same protocol described for the fusion protein, subjecting the proteolytic mixture directly to cellulose affinity chromatography. While thrombin and GST can be removed from the affinity column by extensive washing, CBD binds strongly to the cellulose matrix and can only be eluted with a glucose pulse, similar to XynA and the GST-CBD fusion protein.

Alternatively, all three proteins can be eluted by bidistilled water. However, in the absence of glucose, CBD tends to aggregate during subsequent proteolysis, indicating that the domain is unstable in the absence of glucose or an additional polypeptide chain, here GST. This observation probably explains the difficulties in expressing CBD as distinct entity (W. Liebl, unpubl. results). As a consequence, all measurements of the domain refer to the "holoenzyme," i.e., CBD with bound glucose. The yield of purified CBD, starting from 6 mg fusion protein, was 1.5 mg.

The purification of CBD was followed by SDS-PAGE, as illustrated in Figure 2. Sequence-determination of nine N-terminal residues by Edman degradation was applied to prove the identity and homogeneity of the protein.

Molecular properties

Molecular mass

The molecular mass and the state of association of XynA and CBD were determined by SDS-PAGE, gel-permeation chromatography, and analytical ultracentrifugation (Table 1). Both proteins are monomeric in solution. The higher value for CBD obtained from SDS-PAGE has been reported for other acidic proteins (pI_{CBD} = 4.6), especially polysaccharide hydrolases. Probably, reduced SDS binding is responsible for this artifact (Kaufmann, 1984; Millward-Sadler et al., 1995). Sedimentation velocity experiments showed that XynA sediments as a single symmetrical boundary with a sedimentation coefficient of $s_{20,w}$ = 6.0 ± 0.1 S. In the presence of both 5 M and 7 M GdmCl, the sedimentation coefficient drops to $s_{20,w}$ = 3.3 ± 0.2 S; the relatively large range of error reflects the effect of the denaturant on the partial specific

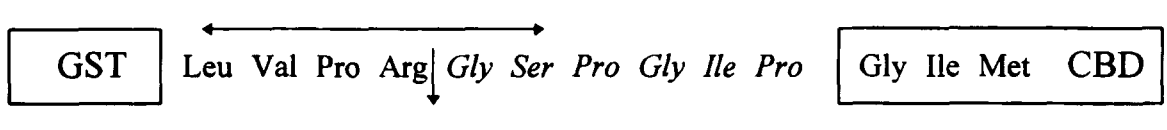

Fig. 1. Schematic map of the GST-CBD fusion protein. Boxes represent the N- and C-terminal proteins. The six-residue extension at the N-terminus of the truncated CBD is presented in italics. The thrombin recognition site and the cleavage site are marked by horizontal and vertical arrows, respectively.

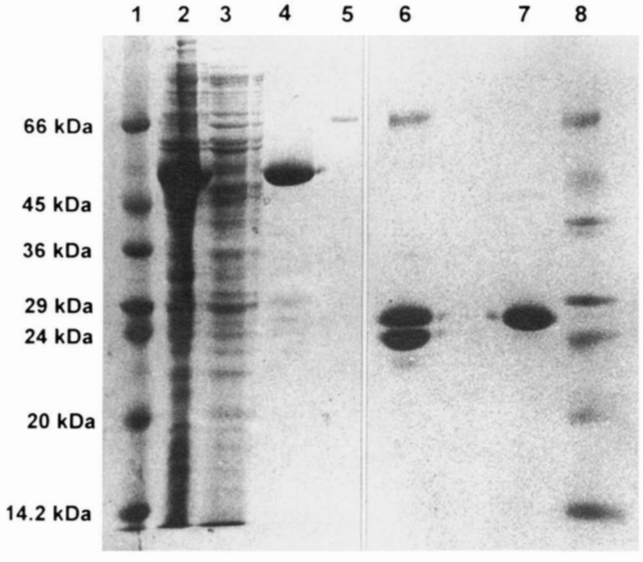

Fig. 2. SDS-PAGE illustrating the purification of CBD. Samples were incubated for 10 min at 95 °C in the presence of 1.25% SDS (w/v) and 2.5% β-mercaptoethanol (v/v). Proteins were stained with Coomassie brilliant blue. Lanes 1 and 8, molecular mass standards: bovine albumin (66 kDa), ovalbumin (45 kDa), glyceraldehyde-3-phosphate dehydrogenase (36 kDa), carbonic anhydrase (29 kDa), trypsinogen (24 kDa), trypsin inhibitor (20 kDa), and α-lactalbumin (14.2 kDa); lane 2, crude extract; lane 3, flow-through from affinity chromatography I; lane 4, pooled fractions from affinity chromatography I (GST-CBD fusion protein); lane 5, thrombin; lane 6, proteolysis of GST-CBD; lane 7, pooled fractions from affinity chromatography II (CBD).

volume and the solvent density (Kawahara & Tanford, 1966; Durchschlag & Jaenicke, 1982). Spectroscopic data clearly show that there is a conformational transition between 5 and 7 M GdmCl (see below); either the change in the hydrodynamic properties in 7 M GdmCl is too small to be detectable by ultracentrifugal analysis, or the increase in solvation and unfolding compensate each other in the given concentration range of GdmCl.

Spectroscopy

The spectroscopic properties of xylanase and CBD, as monitored by UV absorption, fluorescence emission, and circular dichroism, are determined by the high tryptophan and tyrosine content of both proteins (26 Trp, 44 Tyr in the case of XynA; 6 Trp, 7 Tyr for CBD).

UV-absorption. Both proteins show maximum absorbance at 280 nm and shoulders at 290 nm; CBD shows an additional shoulder at 275 nm. The A_{280}/A_{260} ratios for purified XynA and CBD are 1.82 and 1.94 $cm^2 \cdot mg^{-1}$, respectively. The specific extinction coefficients, calculated according to Gill & von Hippel (1989), are 1.72 and 1.98.

Table 1. *Molecular mass of recombinant XynA and CBD from T. maritima*

	XynA (kDa)	CBD (kDa)
Calculated	116.4	22.0
SDS-PAGE	120 ± 7	26 ± 1
Gel-permeation chromatography	114 ± 3	21 ± 1
Sedimentation equilibrium		
0 M GdmCl	120 ± 3	n.d.
7 M GdmCl	116 ± 5	n.d.

Fluorescence. Maximum fluorescence emission (λ_{max}) is observed at an excitation wavelength of 280 nm; λ_{max} for native XynA and CBD are 325 and 330 nm, respectively. Upon denaturation in the presence of 7 M GdmCl, λ_{max} is shifted to 345 and 350 nm. Obviously, XynA retains some residual structure, as indicated by the smaller red shift, as well as its near-UV CD signal (see below).

Circular dichroism. CD spectra of xylanase and its cellulose-binding domain are shown in Figure 3. The far-UV CD of CBD shows maxima at 198 and 230 nm and a minimum at 217 nm. As can be concluded from the comparison with basis spectra obtained for various types of secondary structure, the maximum at 198 nm suggests an antiparallel β-sheet conformation (Perczel et al., 1992). In the isolated fragment, the positive band near 230 nm is probably

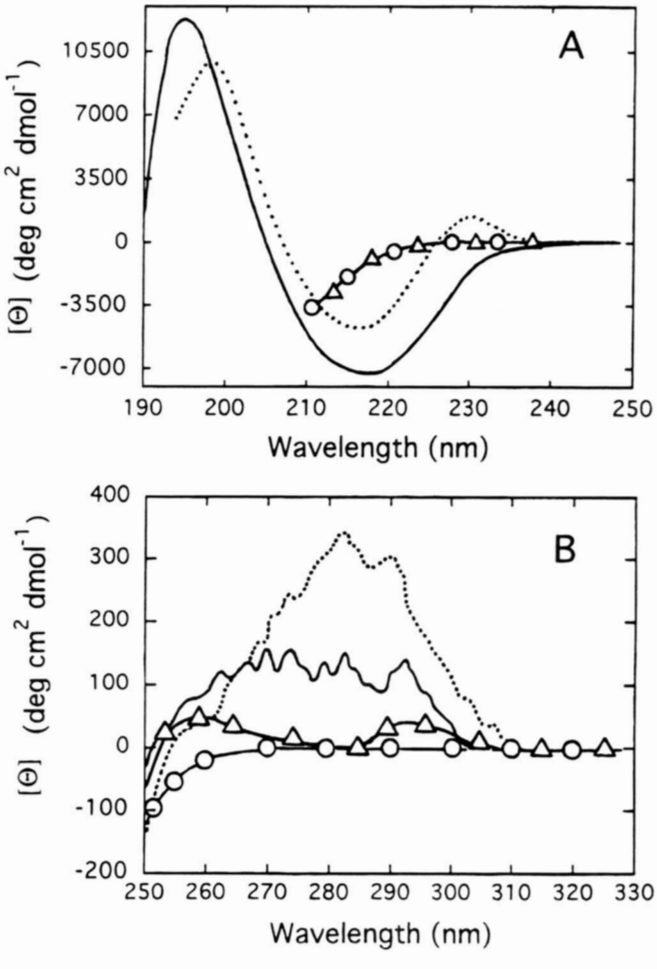

Fig. 3. Circular dichroism spectra of recombinant xylanase XynA and its cellulose-binding domain (CBD). **A:** Far-UV region. **B:** Near-UV region. Protein concentrations 65 and 500 μg/mL, respectively. The spectra of native XynA (——), native CBD (·····), denatured XynA (—△—) and denatured CBD (—○—) were measured in 50 mM sodium phosphate, pH 6.2, and in 7 M GdmCl/50 mM sodium phosphate, pH 6.2, at 20 °C. The spectrum of denatured CBD in the far-UV CD coincides with the one of XynA.

attributable to the contribution of aromatic amino acid residues. This anomaly has been reported for proteins with low α-helical content, in which tryptophan and tyrosine can compensate the negative CD signal of secondary structure (Khan et al., 1989; Woody, 1994).

In contrast to CBD, the far-UV spectrum of xylanase with its maximum at 194 nm and its minimum at 217 nm is indicative for some helicity apart from extended β-strands as expected at least for the catalytic domain with its hypothetical $(\alpha/\beta)_8$-barrel topology (cf. Henrissat, 1991). However, unfolding experiments clearly show that also in the case of xylanase a significant contribution of the aromatic chromophores must be superimposed over the far-UV CD signal of the α-helices (see below). The near-UV spectra for the native enzymes indicate well-ordered tertiary structures with significant differences in shape between XynA and CBD. In 7 M GdmCl, the signal for CBD vanishes; $[\Theta]_\lambda$ for XynA still exhibits minor deviations from zero, indicating some residual asymmetry in the environment of aromatic chromophores. On the other hand, the far-UV CD signal in the presence of 7 M GdmCl suggests both the entire enzyme and its CBD to be unfolded. Obviously, in the case of XynA, the contributions of α-helices and aromatic chromophores cancel each other within the range of error.

GdmCl-induced denaturation

The stability and unfolding of xylanase and CBD was monitored by CD and fluorescence spectroscopy using GdmCl as a denaturant. While fluorescence emission and near-UV CD reflect alterations in tertiary structure, the ellipticity at 220 nm is usually correlated with the α-helical content of a protein.

Xylanase. XynA shows high stability against GdmCl-induced denaturation, even at pH 2.6. Figure 4 illustrates the biphasic unfolding transitions at pH 7.2, 6.2, 4.2, and 2.6, applying fluorescence as well as CD spectroscopy. In the far-UV CD, the major denaturation transition occurs at a GdmCl concentration of about 4.0 M, followed by a second, less pronounced step in the range of 5.1 to 7.0 M GdmCl. Both transitions depend on the pH. This holds especially for the second transition, which shows an increase in $c_{1/2}$(GdmCl) with decreasing pH. Ascribing the bimodal profiles to independent folding domains, this would imply that one part of the protein shows enhanced stability with increasing protonation of its acidic residues.

The differences in ellipticity at zero GdmCl concentration cannot be explained as buffer effects, because the ionic strength does not differ drastically, and at both pH 6.2 and 7.2 phosphate buffer was used. The increase in the negative ellipticity at low pH (cf. Figs. 4,5) might be attributed to an increase in helicity of the protein. A more plausible explanation could be that titration of groups in the pH range between pH 7.2 and pH 4.6, as well as acid denaturation at pH 2.6, affect the tertiary structure to the effect that positive contributions of aromatic residues to the far-UV CD are diminished or quenched. The net result would then be an increase in the negative value of $[\Theta]_{220\ nm}$. Near-UV spectra of XynA at varying pH support this explanation (cf. insert, Fig. 5).

The unfolding transitions, monitored by fluorescence emission, point to a gradual destabilization of the native tertiary structure with decreasing pH (Fig. 4). At neutral pH, low cooperativity prevails; with decreasing pH, bimodal characteristics emerge, with midpoints of the respective unfolding steps shifted to GdmCl concentrations as low as 0.1 M and 3.5 M. At present, no interpretation of the changes in the local environments of the aromatic residues contributing to the different transitions can be given.

Attempts to refold XynA by rapid 20-fold dilution were unsuccessful; the maximum fluorescence emission was not shifted back to the characteristic λ_{max} value observed for the native enzyme. Thus, denaturation transitions using GdmCl do not allow the folding mechanism of XynA to be analyzed.

Cellulose-binding domain. The cellulose-binding domain of XynA shows a GdmCl-induced unfolding transition at $c_{1/2}$(GdmCl) ~4.5 M, making use of far-UV CD ($[\Theta]_{217\,nm}$) at pH 6.2 (Fig. 6). The low cooperativity and the overall complexity of the profile indicate that the unfolding of CBD does not obey a two-state model. As pointed out in connection with XynA, the increase in negative ellipticity in the pretransition region between 0 and 3 M GdmCl may reflect the elimination of contributions of aromatic residues to $[\Theta]_{217\,nm}$, due to local changes in their environment.

Preliminary renaturation experiments, making use of the regain of native fluorescence, showed about 80% reversibility. This demonstrates that the 22-kDa C-terminal part of XynA behaves as an independent folding unit with high intrinsic stability. In this context, it is important to emphasize once more that glucose is essential to prevent aggregation. It remains to be shown whether CBD is part of the most stable unit in the overall unfolding transition of XynA (cf. Fig. 4). The difference in stability ($c_{1/2}$(GdmCl) = 5.6 M and 4.5 M for XynA and CBD, respectively) could be easily explained by the well-established mutual stabilization of substructures in large proteins (Vita et al., 1989; Jaenicke, 1996).

Thermal denaturation

Both the entire xylanase and the truncated domain show high intrinsic stability against thermal unfolding.

Xylanase. In order to monitor the heat stability of XynA, "melting curves" at various GdmCl concentrations were recorded using the far-UV CD at 220 nm as a signal. In the absence of denaturant, the melting point, T_m, of the protein lies beyond 105 °C. With increasing GdmCl concentration, the T_m decreased steadily: In 50 mM sodium phosphate buffer, pH 6.2, in the presence of 1, 2, 3, and 4 M GdmCl, T_m amounts to 94, 83, 74, and 66 °C, respectively (Fig. 7). Since thermal denaturation involves the kinetics of unfolding and aggregation, the transitions depend on the heating rate and the protein concentration. Under all conditions, the reaction was completely irreversible so that a thermodynamic analysis was not feasible. Visible aggregation was observed at pH values close to the isoelectric point (pH 4.8), as well as at pH 6.2 in the presence of 1 M GdmCl.

Cellulose-binding domain. CBD of XynA shows anomalous behavior. Figure 8 illustrates the changes in ellipticity at pH 6.2, in the absence and in the presence of 1 M GdmCl on the one hand, and at pH 3.0 in the absence of GdmCl on the other. Within the temperature range of thermal stability, a constant CD signal is obtained. Beyond T_m, a cooperative increase in the negative amplitude of $[\Theta]_{217}$ is observed. Evidently, this effect does not reflect an increase in helicity; rather, it is attributable to changes in the tertiary interactions of aromatic amino acid side chains. Measurements in the near-UV CD at 283 nm confirm this explanation: the corresponding melting points are identical with the midpoints of

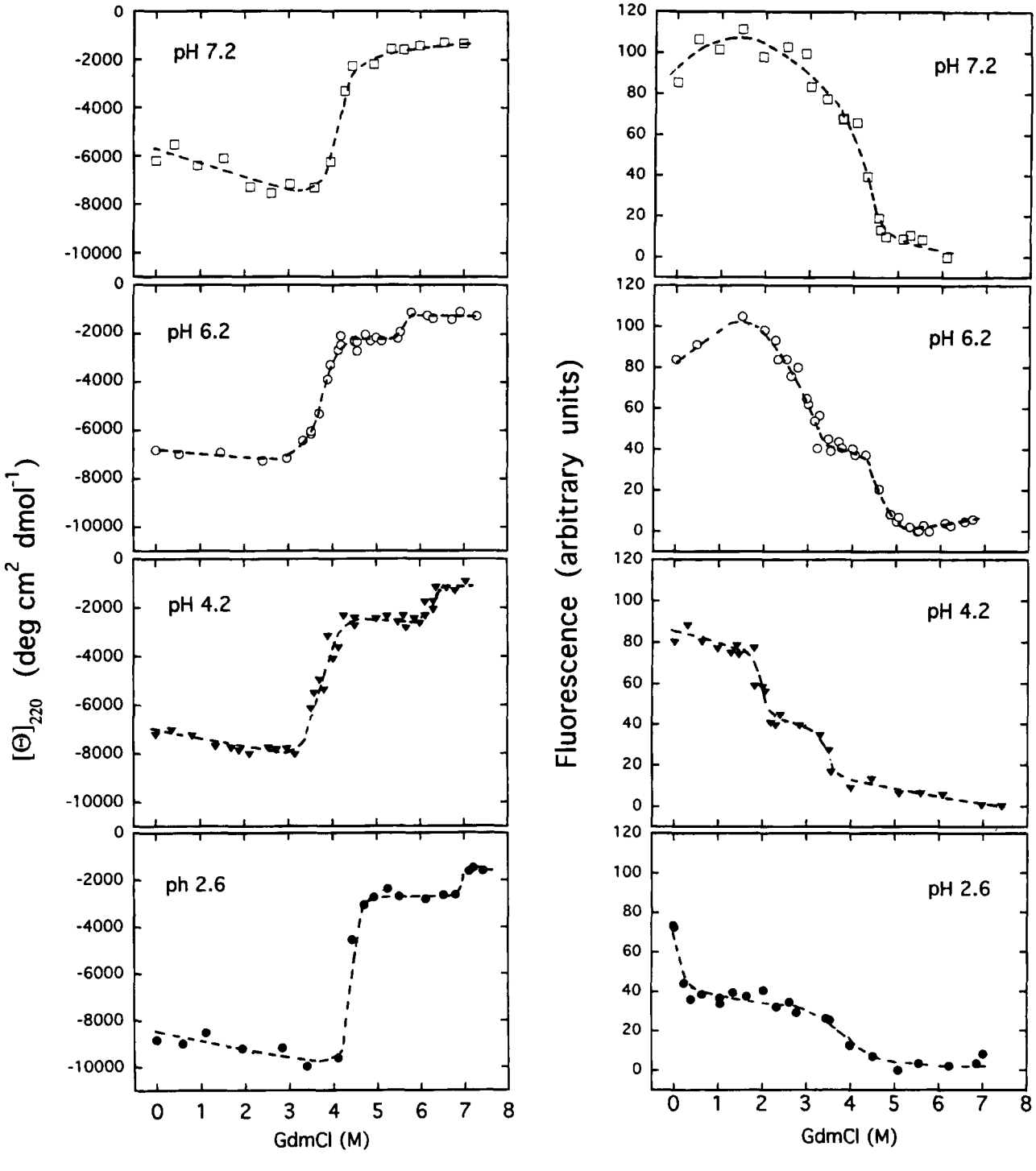

Fig. 4. GdmCl-induced equilibrium transitions of XynA at 20°C, measured by (**A**) far-UV CD at 220 nm and (**B**) fluorescence emission at 317 nm (λ_{exc} = 280 nm). (□) 50 mM sodium phosphate, pH 7.2; (○) 50 mM sodium phosphate, pH 6.2; (▼) 50 mM sodium acetate, pH 4.2; (●) 50 mM citrate phosphate, pH 2.6. Protein concentration: 65 μg/mL for the far-UV CD and 25 μg/mL for fluorescence emission.

the far-UV transitions in Figure 8 (data not shown). The far-UV CD spectra of CBD at temperatures below and above T_m (insert, Fig. 8) reflect the presence of residual secondary structure, suggesting a "molten globule"-like state of the cellulose-binding domain at 80 °C and pH 3.0.

Crystallization

Small crystals of XynA were obtained after one month's growth at room temperature from solutions containing 6 mg/mL protein in 0.1 M HEPES buffer, in the presence of 0.2 M $MgCl_2$ and 30% isopropanol as precipitant. Microseeding led to an increase in size

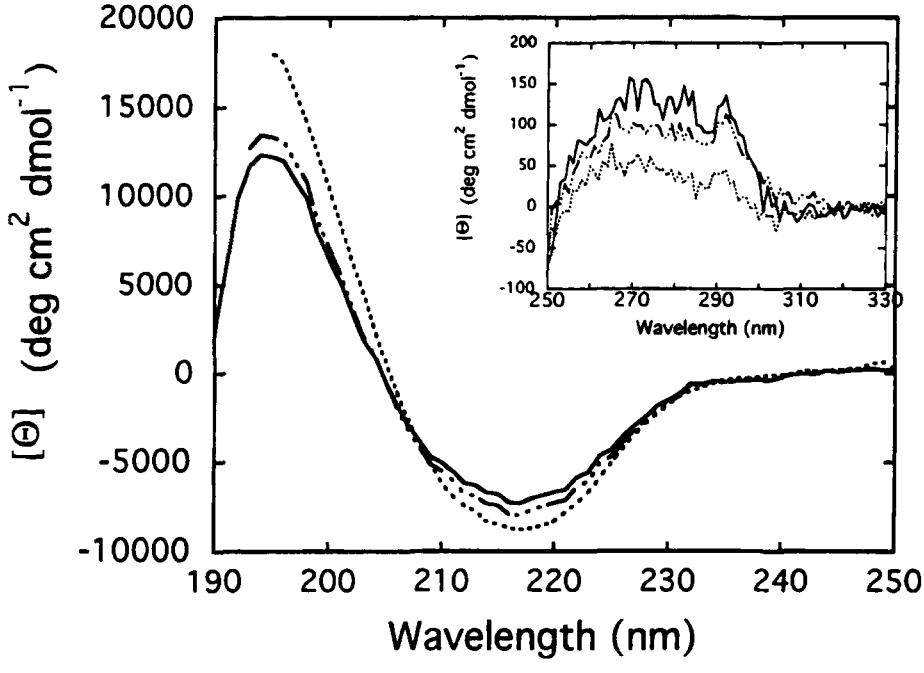

Fig. 5. Far-UV circular dichroism spectra of XynA at 20 °C in 50 mM sodium phosphate, pH 6.2 (——); 50 mM sodium acetate, pH 4.2 (–···–); and 50 mM citrate phosphate, pH 2.6 (·····), at 65 μg/mL. *Insert*: near-UV CD spectra of XynA at 500 μg/mL.

allowing a high resolution data set to be collected (G. Auerbach, pers. comm.).

Conclusions

In the present study, the multidomain protein xylanase, XynA, from the hyperthermophilic bacterium *Thermotoga maritima* was compared with one of its domains, the 22-kDa cellulose-binding domain CBD. In the presence of glucose, this can be cleaved off in its native form from a recombinant glutathione S-transferase fusion protein by proteolysis, thus indicating that it represents a separate folding unit in the intact XynA parent molecule. In the absence of either glucose or the fused polypeptide chain, CBD is unstable, thus explaining the previously observed difficulty in expressing CBD as a distinct entity. As shown by hydrodynamic and chromatographic methods, both XynA and CBD are monomeric in solution.

The spectroscopic comparison of the complete multidomain enzyme and its separate cellulose-binding domain reveals significant

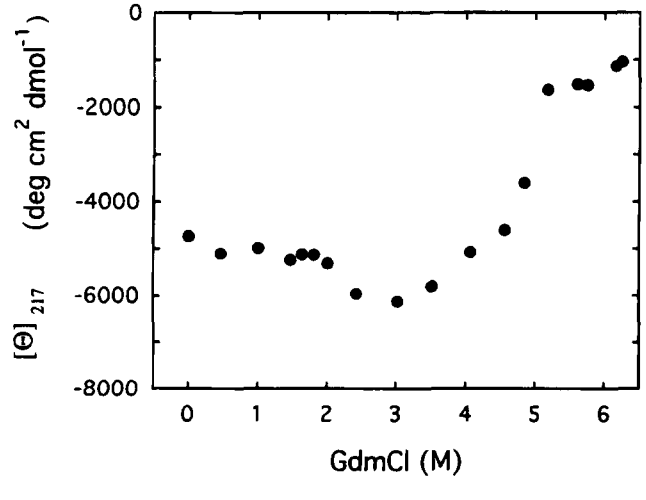

Fig. 6. GdmCl-induced equilibrium transition of CBD at 20 °C, measured by far-UV CD at 217 nm. Protein concentration: 65 μg/mL in 50 mM sodium phosphate, pH 6.2.

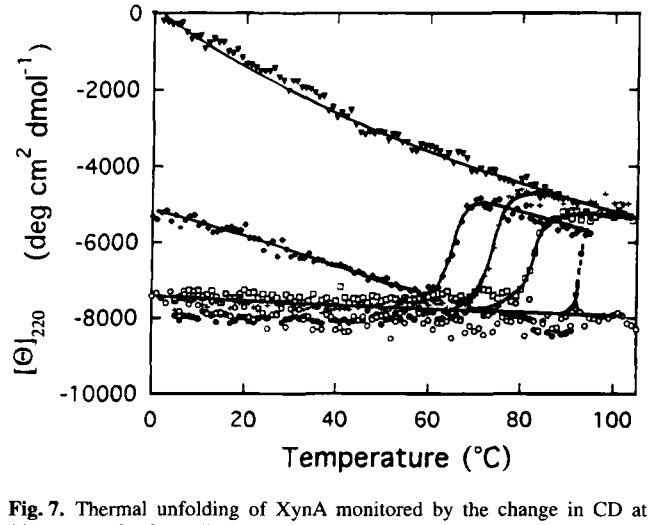

Fig. 7. Thermal unfolding of XynA monitored by the change in CD at 220 nm in 50 mM sodium phosphate, pH 6.2, at varying GdmCl concentrations: (○) 0 M GdmCl; (●) 1 M GdmCl; (□) 2 M GdmCl; (+) 3 M GdmCl; (♦) 4 M GdmCl; (▼) 5 M GdmCl. Protein concentration: 65 μg/mL; heating rate 1 °C/min.

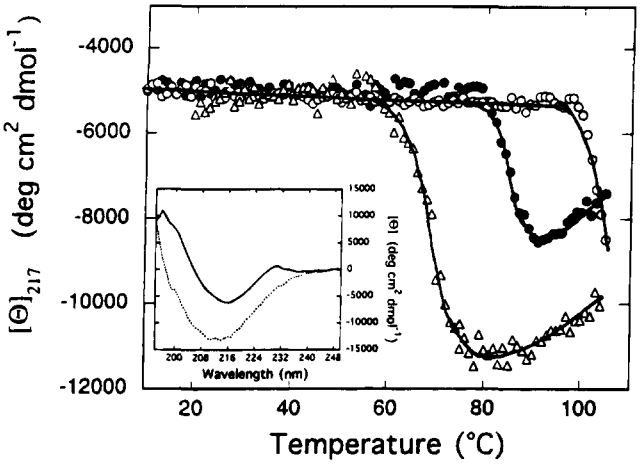

Fig. 8. Thermal unfolding of CBD monitored by the change in CD at 217 nm in different buffer systems: (○) 50 mM sodium phosphate, pH 6.2; (●) in the presence of 1 M GdmCl; (△) and 50 mM glycine/HCl pH 3.0. Heating rate 1 K/min, protein concentration 65 μg/ml. *Insert*: Far-UV CD spectra of CBD in 50 mM glycine/HCl pH 3.0 before (——) and after (·····) thermal unfolding.

differences in the far-UV circular dichroism: XynA shows spectral properties of an α/β protein, whereas CBD with its positive band at 230 nm and the minimum at 218 nm seems to contain mainly β-structure. Both proteins are characterized by far-UV contributions of aromatic residues, which dominate the spectral changes accompanying the unfolding reactions in the presence of denaturants.

Decreasing pH causes a strong increase in negative ellipticity of XynA, suggesting an apparent increase in the helicity. However, monitoring the environment of the aromatic residues by fluorescence emission and near-UV circular dichroism (under the same conditions applied in the far-UV CD measurements), it becomes clear that changes in the tertiary interactions rather than acid denaturation must be involved (Woody, 1994).

The GdmCl-induced unfolding of XynA shows biphasic transitions applying either fluorescence emission or circular dichroism. Upon shifting the pH, the profile of the far-UV CD is altered drastically: The portion of the protein giving rise to the second transition seems to gain stability; the half-concentration is shifted from 5 to 7 M GdmCl. To our knowledge, such a phenomenon has not been described so far. The fact that the transition midpoints derived from the different spectroscopic methods do not coincide points to different unfolding intermediates and clearly contradicts two-state behavior. Thus, quantitative thermodynamic data cannot be obtained from the given spectral data.

As has been mentioned, XynA is assumed to contain five domains. In spite of this multiplicity, only two denaturation steps can be resolved. Similar coupling phenomena in folding/unfolding transitions of domain proteins have been previously reported; they may be explained by mutual stabilization effects (Jaenicke, 1987; Rudolph et al., 1990). In the case of XynA, the fact that the C-terminus with its duplicated cellulose-binding domain is linked to the rest of the protein by a short proline- and threonine-rich stretch suggests the complete 116-kDa molecule to consist of two autonomous folding units coupled by just that connecting peptide.

As observed for all *Thermotoga* proteins investigated so far (Jaenicke et al., 1996), XynA exhibits extremely high intrinsic stability; in the case of CBD, glucose serves as an extrinsic stabilizing factor. The apparent T_m-values of both proteins exceed 100 °C. CBD retains residual secondary structure even at temperatures beyond T_m. In accordance with the high thermal stability, the half-concentrations of the GdmCl-dependent transitions show extreme values. However, the thermal and GdmCl-induced denaturation transitions exhibit significant differences. Similar observations have been reported for other domain proteins (Jaenicke 1987, 1996). Presently, no clear-cut explanation can be given for the divergent mechanisms, because the "unfolded state" of proteins is ill defined, especially comparing the effects of different denaturants. Furthermore, both the explanation of the solubilizing effects of GdmCl on the structure of globular proteins, and the temperature dependence of the stabilizing forces in proteins is still controversial (Eisenberg & Richards, 1995; Makhatadze & Privalov, 1995).

Materials and methods

Materials

Recombinant xylanase XynA was purified as described previously (Winterhalter et al.,1995). Marker proteins for gel-permeation chromatography, thrombin (from bovine plasma), and the protease inhibitor (Pefabloc SC) were purchased from Boehringer (Mannheim). A prepacked Superdex 75 pg-column (1.6 × 60 cm) was purchased from Pharmacia (Uppsala). Ultra-pure GdmCl and microcrystalline cellulose (Avicel PH 105) were products of ICN (Costa Mesa, CA) and Serva (Heidelberg), respectively. All other chemicals were analytical grade substances from Merck (Darmstadt). Quartz-bidistilled water was used throughout.

Purification of GST-CBD

A GST-CBD fusion protein was genetically constructed with a specific thrombin cleavage site as connection; for details see Results and Figure 1. The corresponding plasmid and the bacterial construct *E. coli* XL1 Blue-pGEX-4T-2-C2 have been previously described by Winterhalter et al. (1995). *E. coli* strains were grown at 37 °C in 2 L Luria Bertani medium (1% tryptone, 0.5% yeast extract, 0.5% sodium chloride) with antibiotic selection, to an OD^{600} of about 1; then 1 mM IPTG was added for further incubation. Cells were harvested by centrifugation (4,200 × *g*, 20 min, 4 °C) and resuspended in 50 mM sodium phosphate, pH 6.2, to a calculated optical density of 50. Cell disruption was performed by two passages through an ice-cold French press cell at 18000 psi. After centrifugation (48,200 × *g*, 60 min, 4 °C), the crude extract was loaded onto a microcrystalline cellulose column (2.6 × 12 cm) for 16 h incubation at room temperature. Before this step, the cellulose was pretreated as described by Winterhalter, and the column equilibrated with 20 mM sodium phosphate, pH 6.2/0.5 M NaCl (flow rate 1 mL/min). After washing with equilibration buffer until a constant baseline was reached, the fusion protein was eluted with a pulse of 0.2 M D-(+)-glucose in the same buffer; alternatively, the protein could be eluted with water. The collected fractions were concentrated to about 2 mg/mL and washed with 50 mM sodium phosphate, pH 6.2, by ultrafiltration (Centricon,10 kDa cutoff) in order to remove excess glucose.

Preparation of CBD

Thrombin from bovine plasma was used for cleaving CBD from GST at the genetically engineered site. To this purpose, 6 mg

fusion protein were incubated with 4.6 mg (= 6 U) thrombin in 3 mL 50 mM sodium phosphate buffer, pH 6.2, for 16 h at room temperature. After addition of a protease inhibitor (Pefabloc SC; 0.9 M), the sample was loaded onto a microcrystalline cellulose column (2.6 × 12 cm) equilibrated with 20 mM sodium phosphate/0.5 M NaCl. Thrombin and cleaved GST were removed by extensive washing with the same buffer. Bound CBD was eluted with 0.2 M D-(+)-glucose as mentioned above for the fusion protein. As a consequence, all data for CBD refer to the domain with bound glucose.

Molecular mass

Gel-permeation chromatography

A Superdex 75 pg column (1.6 × 60 cm), equilibrated with 20 mM sodium phosphate buffer, pH 6.2/100 mM NaCl, was used to determine the molecular mass of the isolated domain. Aldolase (158 kDa), bovine serum albumin (68 kDa), ovalbumin (45 kDa), chymotrypsinogen A (25 kDa), and cytochrome c (12.5 kDa) were used as marker proteins.

Sedimentation analysis

Sedimentation velocity and sedimentation equilibrium measurements were performed in a Beckman model E ultracentrifuge equipped with a high-intensity light source and photoelectric scanning system, making use of double sector cells (12 mm) with sapphire windows in an An-G rotor. Scanning wavelength was 280 nm. Sedimentation coefficients were determined at 40,000 rpm, plotting ln r versus time, and correcting for temperature and water viscosity. Sedimentation equilibria were performed at 16,000 rpm; the weight-average molecular mass was calculated from ln c versus r^2 plots making use of a computer program written by G. Böhm (University of Regensburg). The partial specific volume and the solvent density under denaturing conditions were corrected according to Durchschlag & Jaenicke (1982).

SDS-PAGE

SDS-PAGE was carried out using 15% (w/v) acrylamide-gels (Laemmli, 1970). Molecular mass markers were used as described in Figure 2. Gels were stained with Coomassie brilliant blue (Fairbanks et al., 1971).

N-terminal sequencing

Samples were separated on a SDS polyacrylamide gel and transferred onto a polyvinylidene fluoride microporous membrane (Millipore, Zürich). The corresponding Coomassie-stained band was excised from the membrane, and the N-terminus sequenced using an Applied Biosystems Sequencer 477A.

Spectral analysis

Circular dichroism

CD spectra were recorded with an AVIV 62 DS spectropolarimeter at 65 μg/mL (far-UV) and 400–500 μg/mL (near-UV) protein concentration, using 0.1 cm and 1 cm quartz cuvettes, respectively. The bandwidth was 1 nm and the averaging time 20 s/nm. In the case of the GdmCl-induced unfolding transitions, the CD signal of the samples was measured at 220 and 217 nm for XynA and CBD, respectively (1 nm bandwidth, 80 s averaging time). All values were corrected for contributions of the respective solvent. The mean residue ellipticity ([Θ]) was calculated from the measured ellipticity according to Schmid (1989).

UV absorption

UV absorption measurements were performed in an Uvikon 931 spectrophotometer. The extinction coefficients of both xylanase and CBD were determined from the amino acid sequence according to Gill and von Hippel (1989) using the absorbance A_{280} in 7 M GdmCl to correct for denaturation.

Fluorescence emission

Fluorescence was measured on a Perkin-Elmer MPF-3L spectrofluorimeter with 4 nm excitation and 8 nm emission slit widths, λ_{exc} = 280 nm, and a protein concentration of 25 μg/mL. Equilibrium transitions of XynA were monitored at λ_{em} = 317 nm.

Denaturation/renaturation

In order to monitor unfolding equilibrium transitions, samples were incubated at 20 °C for 48 h in the respective buffer at varying GdmCl concentrations, calculated from the refractive index (Pace, 1986). In order to accomplish renaturation, protein denatured in 7 M GdmCl was diluted 20-fold with 50 mM sodium phosphate, pH 6.2, at room temperature. For pH-dependent measurements, 50 mM sodium phosphate (pH 6.2–7.2), 50 mM sodium acetate (pH 4.2), 50 mM glycine-HCl (pH 3.0) and 50 mM citrate-phosphate (pH 2.6) were used. All buffers were titrated to the indicated pH-values at room temperature. In order to monitor thermal denaturation, $[\Theta]_{220\,nm}$ (XynA) and $[\Theta]_{217\,nm}$ (CBD) were recorded at a constant heating rate of 1 °C/min unless noted otherwise. All scans were corrected for solvent effects. The pH of the samples was measured before and after the scans; no changes could be detected.

Crystallization

XynA was crystallized using the hanging drop vapor diffusion method against 0.1 M HEPES/0.2 M $MgCl_2$/30% isopropanol. Growth of large crystals had to be initiated by seeding the droplets with microcrystals grown under identical conditions (see Stura & Wilson, 1990). X-ray intensity data were obtained on an image plate system (MAR Research, Hamburg) mounted on a Rigaku RU200 rotating anode.

Acknowledgments

We thank Drs. R. Glockshuber and F.X. Schmid for critical discussion. N-terminal sequencing was performed by Dr. R. Deutzmann. This work was supported by the Deutsche Forschungsgemeinschaft (Ja 78/34).

References

Amato I. 1993. The crusade against chlorine. *Science 261*:152–154.

Aspinall GO. 1980. Chemistry of cell wall polysaccharides. In: Preiss J, ed. *The biochemistry of plants, vol. 3. Carbohydrates: Structure and function*. New York: Academic Press. pp 473–500.

Black GW, Rixon JE, Clarke JH, Hazlewood GP, Theodorou MK, Morris P, Gilbert HJ. 1996. Evidence that linker sequences and cellulose-binding domains enhance the activity of hemicellulases against complex substrates. *Biochem J 319*:515–520.

Clarke JH, Davidson K, Gilbert HJ, Fontes CMGA, Hazlewood GP. 1996. A modular xylanase from mesophilic *Cellulomonas fimi* contains the same cellulose-binding and thermostabilizing domains as xylanases from thermophilic bacteria. *FEMS Microbiol Lett 139*:27–35.

Durchschlag H, Jaenicke R. 1982. Partial specific volume changes of proteins: Densimetric studies. *Biochem Biophys Res Commun 108*:1074–1079.

Eisenberg DS, Richards FM, eds. 1995. Protein stability. *Adv Prot Chem 46*: 334.

Fairbanks G, Steck TL, Wallach DFH. 1971. Electrophoretic analysis of the major polypeptides of the human erythrocyte membrane. *Biochemistry 10*:2606–2617.

Fontes CMGA, Hazlewood GP, Morag E, Hall J, Hirst BH, Gilbert HJ. 1995. Evidence for a general role for non-catalytic thermostabilizing domains in xylanases from thermophilic bacteria. *Biochem J 307*:151–158.

Gill SJ, von Hippel PH. 1989. Calculation of protein extinction coefficients from amino acid sequence data. *Anal Biochem 182*:319–326.

Henrissat B. 1991. A classification of glycosyl hydrolases based on amino acid sequence similarities. *Biochem J 280*:309–316.

Jaenicke R. 1987. Folding and association of proteins. *Prog Biophys Mol Biol 49*:117–237.

Jaenicke R. 1996. Protein folding and association: In vitro studies for self-organization and targeting in the cell. *Curr Top Cell Regul 34*:209–314.

Jaenicke R, Schurig H, Beaucamp N, Ostendorp R. 1996. Structure and stability of "hyperstable proteins:" Glycolytic enzymes from the hyperthermophilic bacterium *Thermotoga maritima*. *Adv Prot Chem 48*:181–269.

Kantelinen A, Hortling B, Sundquist J, Linko M, Viikari L. 1993. Proposed mechanism of the enzymatic bleaching of kraft pulp with xylanases. *Holzforschung 47*:318–324.

Kaufmann E, Geisler N, Weber K. 1984. SDS-PAGE strongly overestimates the molecular masses of the neurofilament proteins. *FEBS Lett 170*:81–84.

Kawahara K, Tanford C. 1966. Viscosity and density of aqueous solutions of urea and guanidine hydrochloride. *J Biol Chem 241*:3228–3232.

Khan MY, Villanueva G, Newman SA. 1989. On the origin of the positive band in the far-ultraviolet circular dichroic spectrum of fibronectin. *J Biol Chem 264*:2139–2142.

Laemmli UK. 1970. Cleavage of structural proteins during the assembly of the head of bacteriophage T4. *Nature 227*:680–685.

Lee YE, Lowe SE, Henrissat B, Zeikus G. 1993. Characterization of the active site and thermostability regions of endoxylanase from *Thermoanaerobacterium saccharolyticum* B6A-RI. *J Bacteriol 175*:5890–5898.

Makhatadze GI, Privalov PL. 1995. Energetics of protein structure. *Adv Prot Chem 47*:308–425.

Millward-Sadler SJ, Davidson K, Hazlewood GP, Black GW, Gilbert HJ, Clarke JH. 1995. Novel cellulose-binding domains, NodB homologues, and conserved modular architecture in xylanases from the aerobic soil bacteria *Pseudomonas fluorescens* subsp. *cellulosa* and *Cellvibrio mixtus*. *Biochem J 312*:39–48.

Pace CN. 1986. Determination and analysis of urea and guanidine hydrochloride denaturation curves. *Methods Enzymol 131*:266–280.

Perczel A, Park K, Fasman GD. 1992. Deconvolution of the circular dichroism spectra of proteins: The circular dichroism spectra of the antiparallel beta-sheet in proteins. *Proteins Struct Funct Genet 13*:57–69.

Rudolph R, Neßlauer G, Siebendritt R, Sharma AK, Jaenicke R. 1990. Folding of an all-β protein: Independent domain folding in γII-crystallin from calf eye lens. *Proc Natl Acad Sci USA 87*:4625–4629.

Schmid FX. 1989. Spectral methods of characterizing protein conformation and conformational changes. In: Creighton TE, ed. *Protein structure, a practical approach*. Oxford: IRL. pp 251–285.

Stura EA, Wilson IA. 1990. Analytical and production seeding techniques. *Methods: A companion to Methods Enzymol 1*:38–49.

Vita C, Fontana A, Jaenicke R. 1989. Folding of thermolysin fragments. Hydrodynamic properties of isolated domains and subdomains. *Eur J Biochem 183*:513–518.

Whistler RL, Richards EL. 1970. Hemicelluloses. In: Pigman W, Horton D, eds. *The carbohydrates—Chemistry and biochemistry*. New York: Academic Press. pp 447–469.

Winterhalter C, Heinrich P, Candussio A, Wich G, Liebl W. 1995. Identification of a novel cellulose-binding domain within the multidomain 120 kDa xylanase XynA of the hyperthermophilic bacterium *Thermotoga maritima*. *Mol Microbiol 15*:431–444.

Woody RW. 1994. Contributions of tryptophan side chains to the far-ultraviolet circular dichroism of proteins. *Eur Biophys J 23*:253–262.

Zverlov V, Piotukh K, Dakhova O, Velikodvorskaya G, Borriss R. 1996. The multidomain xylanase A of the hyperthermophilic bacterium *Thermotoga neapolitana* is extremely thermoresistant. *Appl Microbiol Biotechnol 45*:245–247.